ACS APPLIED MATERIALS & INTERFACES

Research Article

Cite This: ACS Appl. Mater. Interfaces 2019, 11, 11684−11690

www.acsami.org

Design, Synthesis, and Electrofluorochromism of New Triphenylamine Derivatives with AIE-Active Pendent Groups

Hsiang-Ting Lin,[†,§] Chiao-Ling Huang,[†,§] and Guey-Sheng Liou*[,†,‡]

[†]Institute of Polymer Science and Engineering and [‡]Advanced Research Center for Green Materials Science and Technology, National Taiwan University, Taipei 10617, Taiwan

Supporting Information

ABSTRACT: Triphenylamine (**TPA**) and 4,4′-dimethoxy-triphenylamine (**TPAOMe**) derivatives were successfully linked with two high-performance AIEgens, triphenylethylene (**TPE**) and benzo[*b*]thiophene-1,1-dioxide (**BTO**), to obtain four aggregation-induced emission and electro-active materials, **TPETPA**, **BTOTPA**, **TPETPAOMe**, and **BTOTPAOMe**. The effects on photoluminescence characteristics and electrochromic (EC) and electrofluorochromic (EFC) behaviors in cross-linking gel-type devices derived from the prepared materials were systematically investigated. Furthermore, heptyl viologen was introduced into the EFC devices to enhance EC performance including lower working potential, faster switching time, and superior stability.

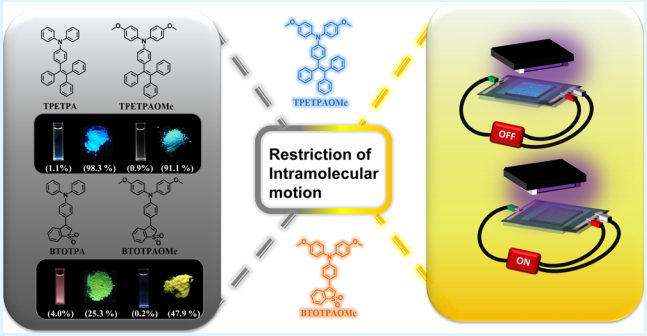

KEYWORDS: *AIE, electrochromism, triphenylamine, electrofluorochromism, triphenylethylene, benzo[b]thiophene-1,1-dioxide*

INTRODUCTION

In 1961, Platt discovered electrochromic (EC) phenomenon which refers to the reversible change in optical absorption upon electrochemical reduction or oxidation.[1] A few years later, Deb published the first electrochromic device (ECD) fabricated by using a WO_3 thin film.[2] To date, numerous EC materials were reported and widely applied in our life, such as adaptive camouflage,[3,4] e-paper,[5,6] smart windows,[7] sunglasses, energy storage devices, and so forth.[8−10] However, the electrochemical properties of fluorescent molecules and devices were overlooked. Until 1993, Lehn et al. proposed a new concept which combines electrochromism and fluorescence in one material called electrofluorochromic (EFC) behavior.[11] Afterward, Audebert and Kim et al. proposed the first paradigm of the electrochemically driven fluorescent device;[12] the photoluminescence (PL) intensity of the device could be changed by electrochemical switching. Nevertheless, serious disadvantage existing in the fabricated device was the result of low PL contrast ratio because of the aggregation-caused quenching (ACQ) effect. To overcome the obstacle, more adaptable materials were designed to fulfill requirements for high-performance EFC devices, such as small organic molecules, polymers, and inorganics.[13−18] Recently, Tang group reported another photophysical phenomenon called aggregation-induced emission (AIE), which is the opposite phenomenon of ACQ, to provide a new avenue and break through the limitation of conventional chromophores. On the basis of this conception, our group designed EFC materials by utilizing AIE/aggregation-enhanced emission polymer containing redox-active triphenylamine (**TPA**) unit and demonstrated excellent performance.[19−23] In order to respond more efficiently and flexibly according to different demands, we therefore try to adopt the concept of utilizing small organic molecules with the redox-active and AIE-active bifunctional characteristics. Although **TPA** displays ACQ property, this study reported that the molecules prepared with the combination of ACQ moiety and AIEgen bring out AIE behavior.[24] In this work, two typical AIEgens were therefore linked to **TPA** and 4,4′-dimethoxy-triphenylamine (**TPAOMe**) to afford novel new AIE-active compounds which could be applied as EFC materials. One of the AIEgens is triphenylethylene (**TPE**), a twist propeller-like structure, leading to the restriction of intramolecular rotations in solid state. Splendid AIE effects of **TPE** derivatives enable to be used in state-of-the-art applications as chemical sensors and organic light-emitting diodes.[25,26] Another one is benzo[*b*]thiophene-1,1-dioxide (**BTO**), a novel AIE core with a ring-fused heterocyclic structure. Owing to its high aromaticity and rich π-electrons of the thiophene moiety, **BTO** derivatives are also good candidates for EFC materials.[27,28] Besides, a novel manufacturing technique was applied for fitting the EFC materials in this study.

EXPERIMENTAL SECTION

Monomer Synthesis and Characterization. Four AIE- and electro-active molecules, consisting of **TPE** or **BTO** core, were

Received: January 11, 2019
Accepted: March 1, 2019
Published: March 1, 2019

DOI: 10.1021/acsami.9b00659
ACS Appl. Mater. Interfaces 2019, 11, 11684−11690

Scheme 1. Synthesis Routes of TPA-Based Luminogens with TPE and BTO AIEgens

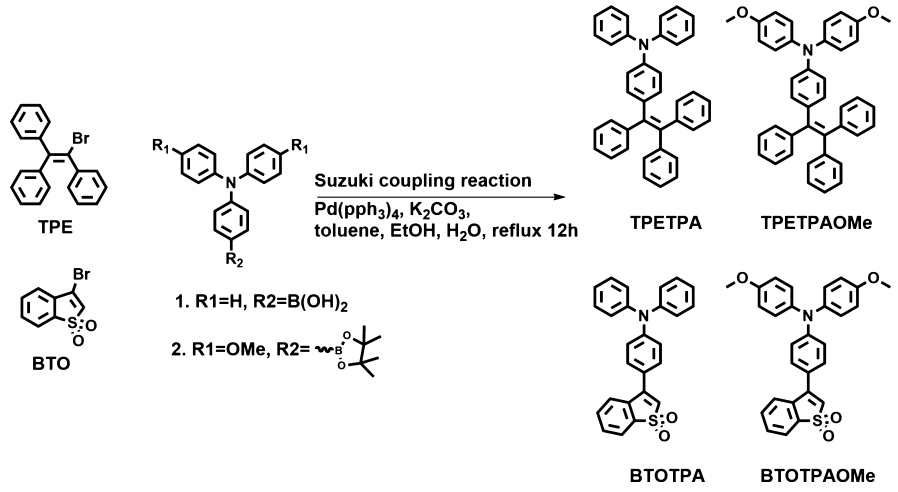

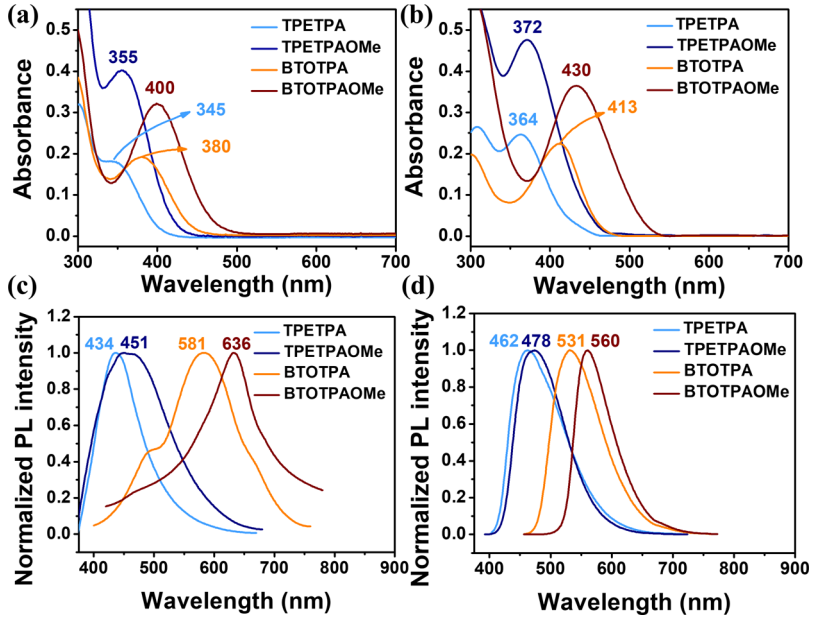

Figure 1. Absorption spectra of four luminogens in (a) NMP solution and (b) solid state. PL spectra of four luminogens in (c) NMP solution and (d) solid state. (Solution concentration: 10 μM.)

synthesized as shown in Scheme 1. **BTO** and **TPE** could be linked with corresponding **TPA**-based boronic acid/ester via Suzuki coupling to generate 1-[(4-diphenylamino)phenyl]-1,2,2-triphenylethene (**TPE-TPA**), 1-[(4-(bis(4-methoxyphenyl)amino)phenyl)]-1,2,2-triphenylethene (**TPE-TPAOMe**), 3-[(4-diphenylamino)-phenyl]-benzo[*b*]thiophene-1,1-dioxide (**BTO-TPA**), and 3-[(4-(bis-(4-methoxyphenyl)amino)phenyl]-benzo[*b*]thiophene-1,1-dioxide (**BTO-TPAOMe**). The details of synthesis procedures and the related NMR spectra are summarized in Supporting Information Schemes S1−S11 and Figures S1−S6.

RESULTS AND DISCUSSION

Optical Properties. The optical properties of these obtained luminogens are depicted in Figure 1a. The maximum absorption (λ_{abs}) of **TPE-TPAOMe** in solution locates at 355 nm, which red-shifts by 10 nm compared to that of **TPE-TPA** (λ_{abs} = 345 nm) because of the electron-donating methoxy functional groups as auxochrome. Approximate results are also observed in **BTO**-based luminogens. Besides, **BTO**-based derivatives show maximum absorption peaks with longer wavelength owing to strong intramolecular charge transfer (ICT) between electron-rich (**TPA**) and electron-deficient (**BTO**) moieties. Similar optical absorption phenomenon of the materials takes place in solid state (Figures 1b, S7, and S8).

PL Properties. These four compounds are almost non-fluorescent in dilute *N*-methyl-2-pyrrolidinone (NMP) solutions. However, greatly enhanced PL emissions could be observed in aggregated state. **TPE-TPA** shows a PL peak at 434 nm with a low fluorescence quantum yield of 1.1%, indicating its weak emitting ability in solution state. Similarly, **TPE-TPAOMe**, **BTO-TPA**, and **BTO-TPAOMe** all exhibit a faint PL peak at 451, 581, and 635 nm with low fluorescence quantum yields of 0.9, 4.0, and 0.2% in NMP solution, respectively (Figure 1c). The fluorescence quantum yield of the compounds could be immensely promoted to 98.3, 91.1, 25.3, and 47.9% in solid state, (Figure 1d). Further, PL behaviors of the four luminogens in different degrees of aggregated state were also investigated as shown in Figure 2. Take **TPE-TPAOMe** as an example, the weak PL signal is

DOI: 10.1021/acsami.9b00659
ACS Appl. Mater. Interfaces 2019, 11, 11684−11690

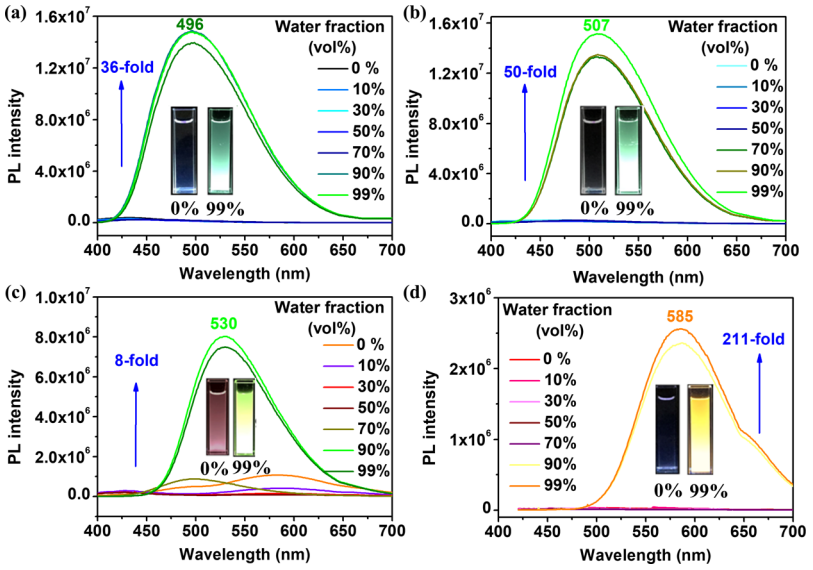

Figure 2. PL spectra based on (a) **TPE-TPA**, (b) **TPE-TPAOMe**, (c) **BTO-TPA**, and (d) **BTO-TPAOMe** in different water/NMP fraction. (Solution concentration: 10 μM.)

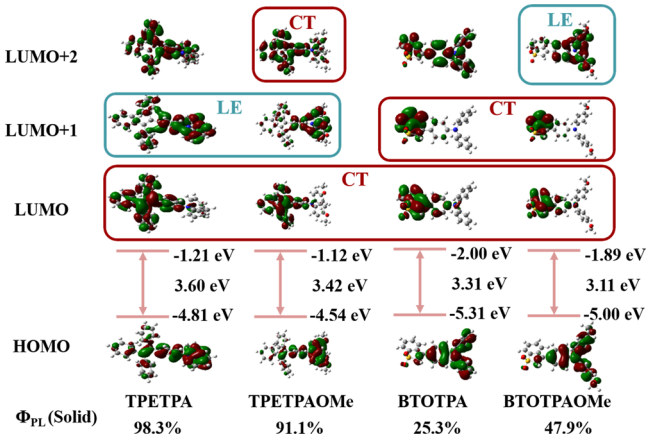

Figure 3. Calculated molecular orbitals of the model compounds (DFT method at B3LYP/6-31G(d)).

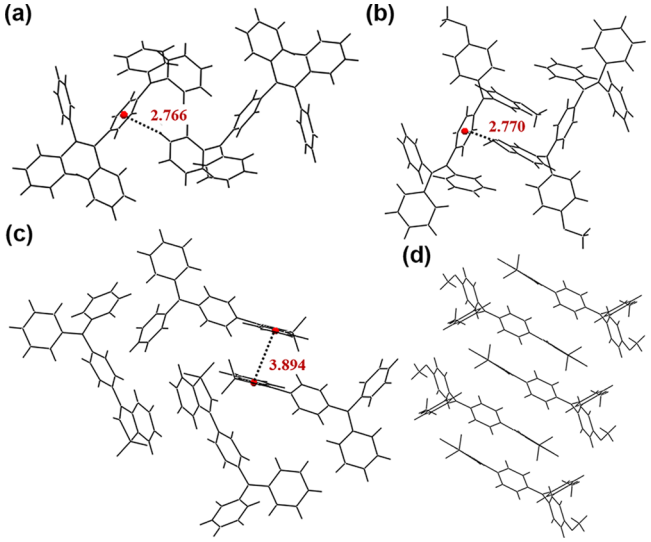

Figure 4. Perspective view of the packing arrangements in the (a) **TPE-TPA**, (b) **TPE-TPAOMe**, (c) **BTO-TPA**, and (d) **BTO-TPAOMe** single crystals.

recorded until the water fraction (f_w) reaches 70% and then sharply increases in the PL intensity. From the NMP dilute solution to the aggregated suspension in the 70% aqueous mixture, maximum emission of the PL intensity increases up to 50-fold in the 99% aqueous mixture. Clearly, **TPE-TPA**, **BTO-TPA**, and **BTO-TPAOMe** all behaved the similar phenomena; especially for **BTO-TPAOMe**, markedly enhancement (211-fold) could be obtained. In dilute solution, the rotation of phenyl rings consumes the energy of the resulted excitons via nonradiative relaxation channels, leading to very low emission.

Table 1. Optical Properties and Energy Levels of Luminogens

	NMP solution			solid powder state				
sample	$\lambda_{abs\ max}$[nm]	$\lambda_{em\ max}$[nm][a]	Φ_{PL} [%][b]	$\lambda_{abs\ max}$[nm]	$\lambda_{em\ max}$[nm][a]	Φ_{PL} [%][c]	α_{AIE}[d]	HOMO/LUMO
TPE-TPA	345	434	1.1	364	462	98.3	89	−4.81/−1.21[e] (−5.28/−2.40)[f]
TPE-TPAOMe	355	451	0.9	372	478	91.1	101	−4.54/−1.12 (−5.06/−2.29)
BTO-TPA	380	581	4.0	412	531	25.3	6	−5.31/−2.00 (−5.43/−2.80)
BTO-TPAOMe	400	630	0.2	433	560	47.9	340	−5.00/−1.89 (−5.17/−2.78)

[a]Both $\lambda_{em\ max}$ of solution and solid states were excited at $\lambda_{abs\ max}$. [b]The quantum yield was measured by using quinine sulfate (dissolved in 1 N H_2SO_4 with a concentration of 10 μM, assuming a PL quantum efficiency of 0.546) as a standard at 25 °C. [c]PL quantum yields of molecules were determined using a calibrated integrating sphere. [d]$\alpha_{AIE} = \Phi_{PL(solid)}/\Phi_{PL(solution)}$. [e]Energy level of luminogens calculated by the DFT method at B3LYP/6-31G(d). [f]Energy level in parentheses is estimated by the experimental data of CV and solid-state UV−vis absorption summarized in Table S1.

DOI: 10.1021/acsami.9b00659
ACS Appl. Mater. Interfaces 2019, 11, 11684−11690

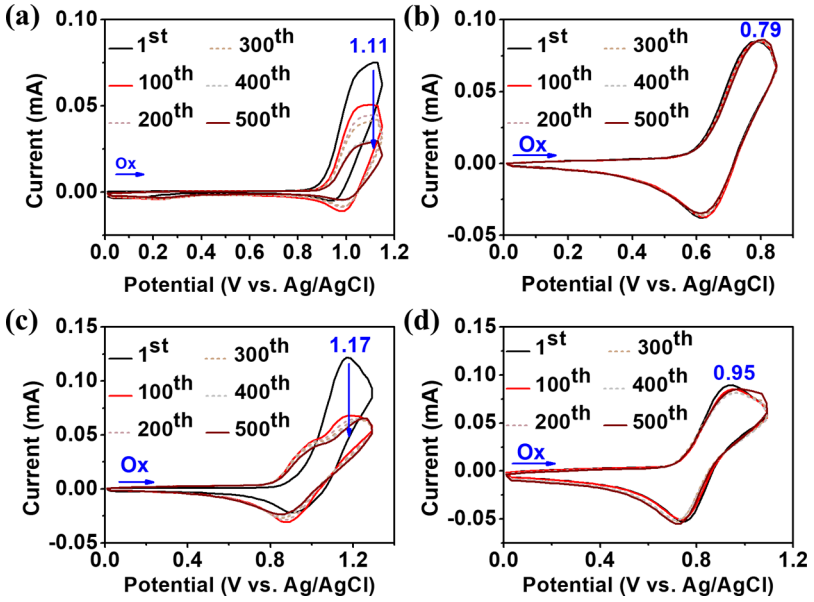

Figure 5. Repetitive CV diagrams of 1 mM (a) **TPE-TPA** in γ-butyrolactone solution, (b) **TPE-TPAOMe**, (c) **BTO-TPA**, and (d) **BTO-TPAOMe** in propylene carbonate (PC) solution for 500 cycles at a scan rate of 50 mV/s, using platinum net as the working electrode and 0.1 M of $TBABF_4$ as the supporting electrolyte.

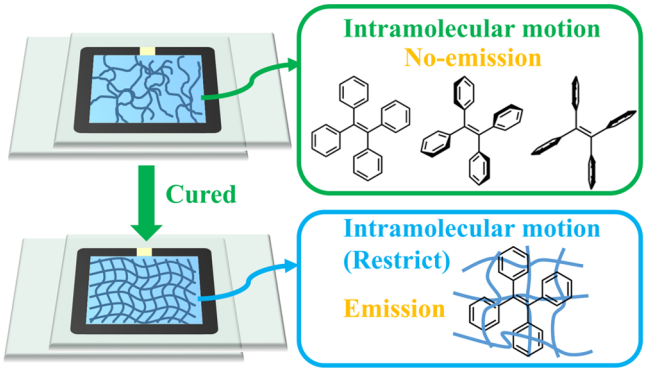

Figure 6. Concept of gel-type EFC devices based on AIE-active EFC materials.

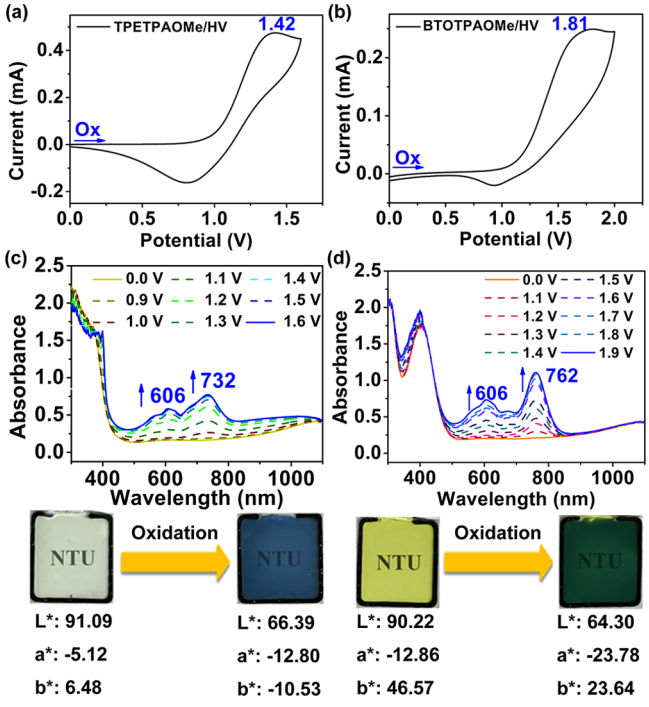

Figure 7. CV diagrams (scan rate: 50 mV/s) based on (a) **TPE-TPAOMe/HV** and (b) **BTO-TPAOMe/HV**. Absorbance spectra based on (c) **TPE-TPAOMe/HV** and (d) **BTO-TPAOMe/HV**. The devices with a gap of 120 μm are prepared from an indium tin oxide (ITO) glass with 2 cm × 2 cm active area.

While the restriction of intramolecular motion (RIM) arises in the aggregated state, causing the molecules to emit intensely.

To comprehend the AIE characteristics in depth, the electronic structures of these luminogens were theoretically calculated by density functional theory (DFT) as shown in Figure 3. The frontier orbitals of highest occupied molecular orbitals (HOMOs) of **TPE-TPA**, **TPE-TPAOMe**, **BTO-TPA**, and **BTO-TPAOMe** mainly locate at the electron-rich moiety, **TPA**, whereas their lowest unoccupied molecular orbitals (LUMOs) mostly center at **TPE** and **BTO** unit. Such a spatial frontier orbital distribution reveals that all of the structures are easy to experience intramolecular charge transfer (ICT) process. In addition, different electronic cloud distributions also appear in LUMO + 1. **TPE**-based luminogens reveal local excited orbital, whereas **BTO**-based derivatives only display charge-transfer orbital transition. This probably causes **TPE**-based luminogens to exhibit higher PL intensity than **BTO**-based derivatives. These optical properties and energy levels have also been summarized in Tables 1 and S1 and Figure S9. Furthermore, the data of geometric structures and packing arrangements of these four luminogens in single crystalline molecules have been summarized and illustrated in Tables S2–S5 and Figure 4.

The C–H···π hydrogen bonds with distances of 2.766 Å shown in Figure 4a could be confirmed between the protons of **TPA** within one molecule of **TPE-TPA** and π-cloud of the **TPA** unit in the neighboring molecule. **TPE-TPAOMe** also exhibits the similar C–H···π interactions (Figure 4b). These so-called C–H···π hydrogen bonds can effectively lock the

DOI: 10.1021/acsami.9b00659
ACS Appl. Mater. Interfaces 2019, 11, 11684–11690

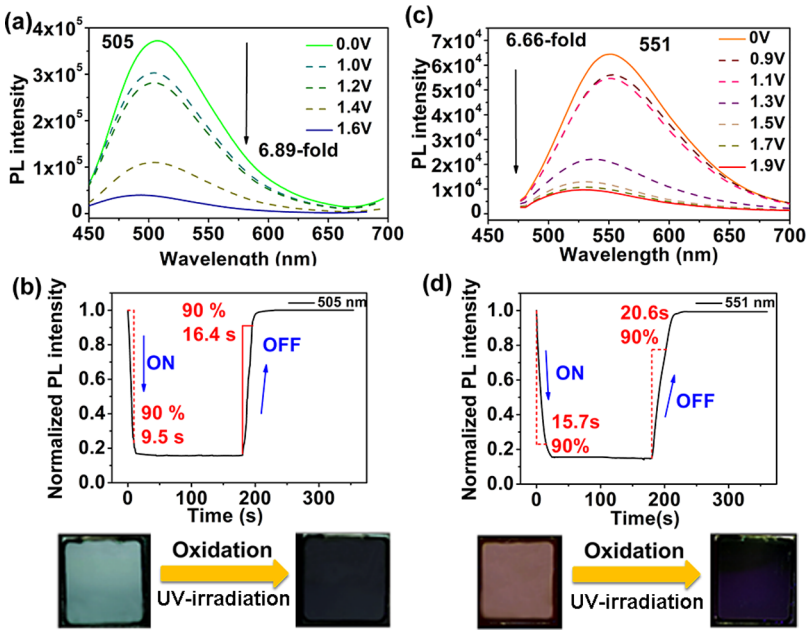

Figure 8. (a,c) PL spectra and (b,d) fluorescence switching of the EFC devices based on (a,b) **TPE-TPAOMe/HV** and (c,d) **BTO-TPAOMe/HV**. The devices with a gap of 120 μm are prepared from the ITO glass with 2 cm × 2 cm active area.

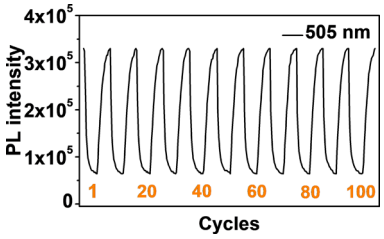

Figure 9. Repetitive switching time test of the EFC device based on **TPE-TPAOMe/HV** between 1.6 V (on) and −0.10 V (off) with a cycle time of 30 s.

RIM to bring about strong emission in solid state. The regular packing arrangements of **BTO-TPA** and **BTO-TPAOMe** (Figure 4c,d) with larger $\pi\cdots\pi$ distances than 3.894 Å could also be observed, indicating that these molecules without the formation of $\pi\cdots\pi$ stacking should be the major reason to enhance the capability to emit in solid state.

Device Fabrication and Properties. Before fabricating the devices, repetitive cyclic voltammetry (**CV**) test is indispensable for confirming the electrochemical stability of the materials. As shown in Figure 5, **TPE-TPAOMe** and **BTO-TPAOMe** demonstrate much higher electrochemical stability than **TPE-TPA** and **BTO-TPA** after 500 CV scanning cycles, indicating that the electron-donating methoxy groups incorporated into the *para*-phenyl position could effectively lower the oxidation potential and obtain stable radical cations without dimerization reactions at these phenyl positions.[29,30] Consequently, **TPE-TPAOMe** and **BTO-TPAOMe** are candidates to be used for fabricating the EFC devices. Afterward, heptyl viologen (**HV**) was also introduced into the system to build an ambipolar system, which enables the resulted devices with lower working voltage, shorter switching response time, enhanced electrochemical stability, and so forth.[31]

In order to fit in with the characteristics of the AIE-active EFC materials, we design and adopt a new technique to fabricate cross-linking gel-type EFC devices which could limit RIM of the AIE-active materials to yield higher PL intensity (Figures 6 and S10). These devices are composed of 0.75 μmol EFC materials and 4 μmol tetrabutylammonium tetrafluoroborate ($TBABF_4$) as the supporting electrolyte in PC or PC/GBL with 7.6 mg poly(MMA-HEMA), 6.3 mg Desmodur N3200, and 0.01 mg dibutyltin diacetate. Particularly, the EFC devices based on **TPE-TPAOMe/HV** are able to be driven without additional supporting electrolyte of $TBABF_4$ (Figure S11) because of the fact that **HV** can also play the role of an electrolyte.[32]

EC and EFC Properties. CV was used to investigate the electrochemical behaviors of EFC devices **TPE-TPAOMe/HV** and **BTO-TPAOMe/HV** in cross-linking gel-type systems, and the representative CV diagrams are shown in Figures 7a and 6b, respectively. **BTO-TPAOMe/HV** (1.80 V) exhibits higher oxidative potential than **TPE-TPAOMe/HV** (1.42 V) because the **BTO** moiety has stronger electron affinity than the **TPE** moiety. Then, the spectroelectrochemical behaviors between the neutral and oxidative states of these two EFC devices are depicted in Figure 7c,d. The **TPE-TPAOMe/HV** device is almost colorless in neutral form (L^*: 91.09; a^*: −5.12; b^*: 6.48) and then the characteristic peaks at around 606 and 732 nm gradually increase; when the applied potential reaches 1.60 V, the device turns blue (L^*: 66.39; a^*: −12.80; b^*: −10.53) corresponding to **TPE-TPAOMe**$^{+\bullet}$**/HV**$^{+\bullet}$. The color of the device based on **BTO-TPAOMe/HV** changes from yellowish (L^*:90.22; a^*: −12.87; b^*: 46.57) to deep yellow-green (L^*: 64.30; a^*: −23.78; b^*: 23.64). The CIE chromaticity diagram and EC switching response are presented in Figures S12−S15 (Supporting Information).

The EFC devices of **TPE-TPAOMe/HV** reveal cyan-blue PL emission with a maximum peak (λ_{em}) at 505 nm under UV excitation. Upon increasing the applied voltage from −0.10 to 1.60 V, the fluorescence of **TPE-TPAOMe/HV** turns to nonemissive dark state. After the applied potential was set back to −0.10 V, it could return back to its original fluorescence state. The PL contrast ratios (I_{off}/I_{on}) of devices derived from **TPE-TPAOMe/HV** and **BTO-TPAOMe/HV** are 6.89 and

DOI: 10.1021/acsami.9b00659
ACS Appl. Mater. Interfaces 2019, 11, 11684−11690

6.66, respectively, as shown in Figures 8a,c and S16. The fluorescence switching response times of **TPE-TPAOMe/HV** and **BTO-TPAOMe/HV** were monitored at 505 and 551 nm, as depicted in Figure 8b,d, respectively, and the **TPE-TPAOMe/HV** device reveals a shorter response time of 9.5 (switching on) and 16.4 s (bleaching off) than those of 15.7 (switching on) and 20.6 s (bleaching off) for the **BTO-TPAOMe/HV** device. The switching tests with different cyclic times have also been conducted, and the obtained results are illustrated in Figure S17. Finally, the long-term stability and reversibility of the resulted EFC devices were investigated by measuring the PL intensity as a function of switching cycles as depicted in Figures 9 and S18. The EFC device based on **TPE-TPAOMe/HV** displays 98% of PL recovery after 100 cycles, indicating high electrochemical switching stability.

CONCLUSIONS

In summary, four AIE-active and EC bifunctional materials, **TPE-TPA**, **TPE-TPAOMe**, **BTO-TPA**, and **BTO-TPAOMe**, were successfully synthesized. All the obtained materials exhibit high quantum yield in solid state (**TPE-TPA**: 98.3%, **TPE-TPAOMe**: 91.1%, **BTO-TPA**: 25.3%, and **BTO-TPAOMe**: 47.9%) and nearly nonemissive in solution state, which is beneficial to many applications. **TPE-TPAOMe** and **BTO-TPAOMe** with the protecting group display excellent electrochemical stability, and then both of them were chosen to be candidates for fabricating EFC devices. In the light of their AIE characteristic, the cross-linking gel-type EFC devices with **HV** were applied for obtaining better performance, and the PL contrast ratio of EFC based on **TPE-TPAOMe/HV** and **BTO-TPAOMe/HV** could be reached to 6.89 and 6.66, respectively. The recovery of the EFC device based on **TPE-TPAOMe/HV** could maintain 98% after 100 cycles, which demonstrates that the AIE- and electro-active bifunctional small molecules could be a feasible approach in the application of EFC devices.

ASSOCIATED CONTENT

Supporting Information

The Supporting Information is available free of charge on the ACS Publications website at DOI: 10.1021/acsami.9b00659.

Experiment details including measurement, monomer synthesis, and monomer characterization and basic EC properties of ECDs derived from **TPE-TPAOMe** and **BTO-TPAOMe** in the ambipolar system (PDF)

Switching behavior of the EFC device (AVI)

AUTHOR INFORMATION

Corresponding Author

*E-mail: gsliou@ntu.edu.tw

ORCID

Guey-Sheng Liou: 0000-0003-3725-3768

Author Contributions

§H.-T.L. and C.-L.H. contributed equally to this work.

Notes

The authors declare no competing financial interest.

ACKNOWLEDGMENTS

This work was financially supported by the "Advanced Research Center for Green Materials Science and Technology" from The Featured Area Research Center Program within the framework of the Higher Education Sprout Project by the Ministry of Education (107L9006) and the Ministry of Science and Technology in Taiwan (MOST 107-3017-F-002-001 and 107-2113-M-002-024-MY3).

REFERENCES

(1) Platt, J. R. Electrochromism, a Possible Change of Color Producible in Dyes by an Electric Field. *J. Chem. Phys.* **1961**, *34*, 862–863.

(2) Deb, S. K. A Novel Electrophotographic System. *Appl. Opt.* **1969**, *8*, 192–195.

(3) Beaupré, S.; Breton, A.-C.; Dumas, J.; Leclerc, M. Multicolored Electrochromic Cells Based On Poly(2,7-Carbazole) Derivatives For Adaptive Camouflage. *Chem. Mater.* **2009**, *21*, 1504–1513.

(4) Yu, H.; Shao, S.; Yan, L.; Meng, H.; He, Y.; Yao, C.; Xu, P.; Zhang, X.; Hu, W.; Huang, W. Side-Chain Engineering of Green Color Electrochromic Polymer Materials: Toward Adaptive Camouflage Application. *J. Mater. Chem. C* **2016**, *4*, 2269–2273.

(5) Kobayashi, N.; Miura, S.; Nishimura, M.; Urano, H. Organic Electrochromism for a New Color Electronic Paper. *Sol. Energy Mater. Sol. Cells* **2008**, *92*, 136–139.

(6) Malti, A.; Brooke, R.; Liu, X.; Zhao, D.; Ersman, P. A.; Fahlman, M.; Jonsson, M. P.; Berggren, M.; Crispin, X. Freestanding Electrochromic Paper. *J. Mater. Chem. C* **2016**, *4*, 9680–9686.

(7) Baetens, R.; Jelle, B. P.; Gustavsen, A. Properties, Requirements and Possibilities of Smart Windows for Dynamic Daylight and Solar Energy Control in Buildings: A State-of-the-Art Review. *Sol. Energy Mater. Sol. Cells* **2010**, *94*, 87–105.

(8) Österholm, A. M.; Shen, D. E.; Kerszulis, J. A.; Bulloch, R. H.; Kuepfert, M.; Dyer, A. L.; Reynolds, J. R. Four Shades of Brown: Tuning of Electrochromic Polymer Blends Toward High-Contrast Eyewear. *ACS Appl. Mater. Interfaces* **2015**, *7*, 1413–1421.

(9) Hee, W. J.; Alghoul, M. A.; Bakhtyar, B.; Elayeb, O.; Shameri, M. A.; Alrubaih, M. S.; Sopian, K. The Role of Window Glazing on Daylighting and Energy Saving in Buildings. *Renewable Sustainable Energy Rev.* **2015**, *42*, 323–343.

(10) Tong, Z.; Tian, Y.; Zhang, H.; Li, X.; Ji, J.; Qu, H.; Li, N.; Zhao, J.; Li, Y. Recent Advances in Multifunctional Electrochromic Energy Storage Devices and Photoelectrochromic Devices. *Sci. China: Chem.* **2017**, *60*, 13–37.

(11) Goulle, V.; Harriman, A.; Lehn, J.-M. An Electro-photoswitch: Redox Switching of the Luminescence of a Bipyridine Metal Complex. *J. Chem. Soc., Chem. Commun.* **1993**, *6*, 1034–1036.

(12) Kim, Y.; Kim, E.; Clavier, G.; Audebert, P. New Tetrazine-Based Fluoroelectrochromic Window; Modulation of the Fluorescence through Applied Potential. *Chem. Commun.* **2006**, 3612–3614.

(13) Yuan, Y.-X.; Chen, Y.; Wang, Y.-C.; Su, C.-Y.; Liang, S.-M.; Chao, H.; Ji, L.-N. Redox responsive luminescent switch based on a ruthenium(II) complex $[Ru(bpy)_2(PAIDH)]^{2+}$. *Inorg. Chem. Commun.* **2008**, *11*, 1048–1050.

(14) Seo, S.; Kim, Y.; Zhou, Q.; Clavier, G.; Audebert, P.; Kim, E. White Electrofluorescence Switching from Electrochemically Convertible Yellow Fluorescent Dyad. *Adv. Funct. Mater.* **2012**, *22*, 3556–3561.

(15) Audebert, P.; Miomandre, F. Electrofluorochromism: from molecular systems to set-up and display. *Chem. Sci.* **2013**, *4*, 575–584.

(16) Kanazawa, K.; Nakamura, K.; Kobayashi, N. High-Contrast Electroswitching of Emission and Coloration Based on Single-Molecular Fluoran Derivatives. *J. Phys. Chem. A* **2014**, *118*, 6026–6033.

(17) Al-Kutubi, H.; Zafarani, H. R.; Rassaei, L.; Mathwig, K. Electrofluorochromic Systems: Molecules and Materials Exhibiting Redox-Switchable Fluorescence. *Eur. Polym. J.* **2016**, *83*, 478–498.

(18) Kanazawa, K.; Nakamura, K.; Kobayashi, N. Electroswitchable Optical Device Enabling both Luminescence and Coloration Control Consisted of Fluoran Dye and 1,4-Benzoquinone. *Sol. Energy Mater. Sol. Cells* **2016**, *145*, 42–53.

DOI: 10.1021/acsami.9b00659
ACS Appl. Mater. Interfaces 2019, 11, 11684–11690

(19) Ning, Z.; Chen, Z.; Zhang, Q.; Yan, Y.; Qian, S.; Cao, Y.; Tian, H. Aggregation-Induced Emission (AIE)-active Starburst Triarylamine Fluorophores as Potential Non-doped Red Emitters for Organic Light-Emitting Diodes and Cl_2 Gas Chemodosimeter. *Adv. Funct. Mater.* **2007**, *17*, 3799−3807.
(20) Ning, Z.; Tian, H. Triarylamine: A Promising Core Unit for Efficient Photovoltaic Materials. *Chem. Commun.* **2009**, *37*, 5483−5495.
(21) Yen, H.-J.; Chen, C.-J.; Liou, G.-S. Novel High-Efficiency PL Polyimide Nanofiber Containing Aggregation-Induced Emission (AIE)-Active Cyanotriphenylamine Luminogen. *Chem. Commun.* **2013**, *49*, 630−632.
(22) Wu, J.-H.; Liou, G.-S. High-Performance Electrofluorochromic Devices Based on Electrochromism and Photoluminescence-Active Novel Poly(4-Cyanotriphenylamine). *Adv. Funct. Mater.* **2014**, *24*, 6422−6429.
(23) Cheng, S.-W.; Han, T.; Huang, T.-Y.; Tang, B.-Z.; Liou, G.-S. High-Performance Electrofluorochromic Devices Based on Aromatic Polyamides with AIE-active Tetraphenylethene and Electro-active Triphenylamine Moieties. *Polym. Chem.* **2018**, *9*, 4364−4373.
(24) Yuan, W. Z.; Lu, P.; Chen, S.; Lam, J. W. Y.; Wang, Z.; Liu, Y.; KwoK, H. S.; Ma, Y.; Tang, B. Z. Changing the Behavior of Chromophores from Aggregation-Caused Quenching to Aggregation-Induced Emission: Development of Highly Efficient Light Emitters in the Solid State. *Adv. Mater.* **2010**, *22*, 2159−2163.
(25) Liu, Y.; Chen, X.; Lv, Y.; Chen, S.; W. Y. Lam, J.; Mahtab, F.; Kwok, H. S.; Tao, X.; Tang, B. Z. Systemic Studies of Tetraphenylethene-Triphenylamine Oligomers and a Polymer: Achieving Both Efficient Solid-State Emissions and Hole-Transporting Capability. *Chem.—Eur. J.* **2012**, *18*, 9929−9938.
(26) Chan, C. Y. K.; Lam, J. W. Y.; Zhao, Z.; Chen, S.; Lu, P.; Sung, H. H. Y.; Kwok, H. S.; Ma, Y.; Williams, I. D.; Tang, B. Z. Aggregation-Induced Emission, Mechanochromism and Blue Electroluminescence of Carbazole and Triphenylamine-Substituted Ethenes. *J. Mater. Chem. C* **2014**, *2*, 4320−4327.
(27) Guo, J.; Hu, S.; Luo, W.; Hu, R.; Qin, A.; Zhao, Z.; Tang, B. Z. A Novel Aggregation-Induced Emission Platform from 2,3-Diphenylbenzo[b]thiophene S,S-Dioxide. *Chem. Commun.* **2017**, *53*, 1463−1466.
(28) Zhen, S.; Guo, J.; Luo, W.; Qin, A.; Zhao, Z.; Tang, B. Z. Synthesis, Structure, Photoluminescence and Photochromism of Phosphindole Oxide and Benzo[b]thiophene S,S-Dioxide Derivatives. *J. Photochem. Photobiol., A* **2018**, *355*, 274−282.
(29) Chang, C.-W.; Liou, G.-S.; Hsiao, S.-H. Highly Stable Anodic Green Electrochromic Aromatic Polyamides: Synthesis and Electrochromic Properties. *J. Mater. Chem.* **2007**, *17*, 1007−1015.
(30) Liou, G.-S.; Lin, H.-Y. Synthesis and Electrochemical Properties of Novel Aromatic Poly(amine−amide)s with Anodically Highly Stable Yellow and Blue Electrochromic Behaviors. *Macromolecules* **2009**, *42*, 125−134.
(31) Yen, H.-J.; Liou, G.-S. Design and Preparation of Triphenylamine-Based Polymeric Materials Towards Emergent Optoelectronic Applications. *Prog. Polym. Sci.* **2019**, *89*, 250−287.
(32) Wu, J.-T.; Liou, G.-S. A Novel Panchromatic Shutter Based on an Ambipolar Electrochromic System without Supporting Electrolyte. *Chem. Commun.* **2018**, *54*, 2619−2622.

DOI: 10.1021/acsami.9b00659
ACS Appl. Mater. Interfaces 2019, 11, 11684−11690